Lead Optimization of P5U and Urantide: Discovery of Novel Potent Ligands at Urotensin-II Receptor.

ARTICLE *in* JOURNAL OF MEDICINAL CHEMISTRY · JULY 2014

Impact Factor: 5.45 · DOI: 10.1021/jm500218x · Source: PubMed

13 AUTHORS, INCLUDING:

Daniela Marasco
University of Naples Federico II
86 PUBLICATIONS **916** CITATIONS
SEE PROFILE

Pietro Campiglia
Università degli Studi di Salerno
143 PUBLICATIONS **1,333** CITATIONS
SEE PROFILE

Isabel M Gomez-Monterrey
University of Naples Federico II
99 PUBLICATIONS **1,945** CITATIONS
SEE PROFILE

Paolo Grieco
University of Naples Federico II
179 PUBLICATIONS **2,366** CITATIONS
SEE PROFILE

Journal of Medicinal Chemistry

Article

pubs.acs.org/jmc

Lead Optimization of P5U and Urantide: Discovery of Novel Potent Ligands at the Urotensin-II Receptor

Alfonso Carotenuto,[†] Luigia Auriemma,[†] Francesco Merlino,[†] Ali Munaim Yousif,[†] Daniela Marasco,[†,‡] Antonio Limatola,[†] Pietro Campiglia,[∥] Isabel Gomez-Monterrey,[†] Paolo Santicioli,[§] Stefania Meini,[§] Carlo A. Maggi,[§] Ettore Novellino,[†] and Paolo Grieco*[,†,‡]

[†]Department of Pharmacy, University of Naples "Federico II", I-80131 Naples, Italy

[‡]CIRPEB: Centro Interuniversitario di Ricerca sui Peptidi Bioattivi , University of Naples "Federico II", DFM-Scarl, Institute of Biostructures and Bioimaging-CNR, 80134, Naples, Italy

[§]Department of Pharmacology, Menarini Ricerche, Via Rismondo 12/A, I-50131, Florence, Italy

[∥]Department of Pharmacy, University of Salerno, I-84084 Fisciano, Salerno Italy

S *Supporting Information*

ABSTRACT: We have optimized **1** (P5U) and urantide, two important ligands at the *h*-UT receptor, designing several analogues by the exchange of the Tyr[9] residue with different unnatural aromatic amino acids. This study allowed us to discover novel ligands with improved activity. In particular, the replacement of the Tyr[9] residue by (pCN)Phe or (pNO_2)Phe within the urantide sequence led to compounds **13** (UPG-83) and **15** (UPG-95), respectively, which showed pure antagonist activity toward UT receptor in a rat aorta bioassay. More interestingly, the replacement of the Tyr[9] in **1** sequence with the Btz or the (3,4-Cl)Phe residues led to superagonists **6** (UPG-100) and **10** (UPG-92) with pEC_{50} values at least 1.4 log higher than that of **1**, being the most potent UT agonists discovered to date. Compounds **10** and **13** showed also a good stability in a serum proteolytic assay. These ligands represent new useful tools to further characterize the urotensinergic system in human physiopathology.

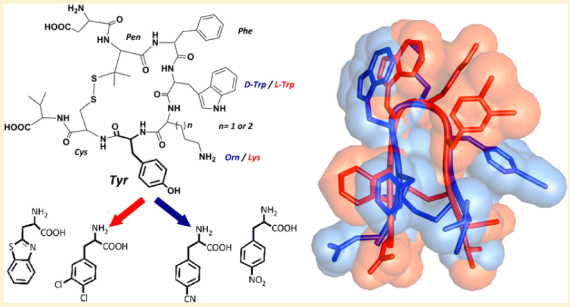

INTRODUCTION

Urotensin-II (U-II), a somatostatin-like neuropeptide, is a cyclic peptide originally isolated in the teleost fish *Gillichthys mirabilis* in the 1960s.[1] Subsequently, it has been demonstrated that U-II is also expressed in tetrapods and that its gene is located in the central nervous system (CNS).[2] The human U-II (*h*U-II) consists of 11 amino acids, H-Glu-Thr-Pro-Asp-c[Cys-Phe-Trp-Lys-Tyr-Cys]-Val-OH, and the whole sequence is recognized as the natural ligand of an orphan rat G-protein coupled receptor, first named GPR14.[3,4] Subsequently, a human G-protein coupled receptor with 75% similarity to the orphan rat receptor was replicated and finally renamed the UT receptor by IUPHAR.[5] The U-II precursor has proved to be widely expressed in various vertebrate species, including frogs, rats, mice, pigs, monkeys, and humans.[6]

In 2003, a paralogue of U-II, known as urotensin-related peptide (URP), was isolated in mammals.[7] The U-II and URP genes are mostly expressed in motoneurons located in discrete brainstem nuclei and in the ventral horn of the spinal cord.[6] U-II and URP mRNAs have also been detected, albeit in lower concentrations, in different peripheral tissues, including the pituitary, heart, spleen, thymus, pancreas, kidney, small intestine, adrenal gland, and prostate.[6] Also, UT receptor is widely distributed in the CNS and in different organs and peripheral tissues, including cardiovascular system, kidney, bladder, prostate, and adrenal gland.[3,8−10] This extensive expression turned out to be very important in understanding the multiple pathophysiological effects in which the *h*U-II/UT receptor interaction is involved, such as cardiovascular disorders (heart failure, cardiac remodelling, hypertension), smooth muscle cell proliferation, renal disease, diabetes, and tumor growth.[11]

It has recently been reported that U-II plays an important role in pulmonary hypertension,[12] modulates erectile function through eNOS,[13] and regulates cell proliferation in prostate cancer.[14] Furthermore, it has been demonstrated that U-II is implicated in immune inflammatory diseases[15] and in many effects on the CNS.[16] Hence, *h*U-II analogues could be therapeutically appealing in diverse pathological disorders.[17]

The N-terminus portion of urotensin isopeptides is highly variable across animal species,[18] whereas the C-terminal region, structurally organized in a cyclic sequence by a disulfide bridge, c[Cys-Phe-Trp-Lys-Tyr-Cys], is well-conserved from species to species, outlining its primary role in the biological activity.[19] In fact, the conserved C-terminal octapeptide cyclic portion of U-II [*h*U-II(4−11)] retains both biological and binding properties.

Received: February 10, 2014

   dx.doi.org/10.1021/jm500218x | *J. Med. Chem.* XXXX, XXX, XXX−XXX

Table 1. Receptor Affinity and Biological Activity of 1 and Urantide Analogues of the General Formula H-Asp-c[Pen[a]-Phe-*Xaa*-*Yaa*-R-Cys]-Val-OH

peptide	Xaa	Yaa	R[g]	pK_i[b]	pEC_{50}[c]	E_{max}[d]	pK_B[e]
*h*U-II[f]	Trp	Lys	Tyr	9.10 ± 0.08	8.50 ± 0.06	100	nd
*h*U-II(4−11)	Trp	Lys	Tyr	9.60 ± 0.07	8.44 ± 0.03	100	nd
1	Trp	Lys	Tyr	9.70 ± 0.070	9.4 ± 0.2[j]	95 ± 7	nd
urantide	DTrp	Orn	Tyr	8.30 ± 0.04	na	0.0	8.32 ± 0.10
2	Trp	Lys	(2)Nal	8.70 ± 0.08	9.14 ± 0.06[j]	85 ± 16	nd
3	DTrp	Orn	(2)Nal	9.14 ± 0.08	8.42 ± 0.17	13 ± 5[h]	nd
4	Trp	Lys	(1)Nal	9.40 ± 0.07	8.3 ± 0.2[i]	86 ± 5	nd
5	DTrp	Orn	(1)Nal	8.19 ± 0.14	7.74 ± 0.10[j]	37 ± 9[h]	nd
6	Trp	Lys	Btz	8.76 ± 0.11	10.71 ± 0.04[i,j]	89 ± 16	nd
7	DTrp	Orn	Btz	7.89 ± 0.13	7.47 ± 0.11[j]	57 ± 2[h]	nd
8	Trp	Lys	(pCl)Phe	8.91 ± 0.07	9.09 ± 0.12[j]	85 ± 10	nd
9	DTrp	Orn	(pCl)Phe	8.98 ± 0.05	8.57 ± 0.18	13 ± 3[h]	nd
10	Trp	Lys	(3,4-Cl)Phe	9.11 ± 0.06	10.9 ± 0.14[i,j]	102 ± 8	nd
11	DTrp	Orn	(3,4-Cl)Phe	8.65 ± 0.09	7.89 ± 0.17[j]	26 ± 7[h]	nd
12	Trp	Lys	(pCN)Phe	8.74 ± 0.10	8.97 ± 0.15	79 ± 1[h]	nd
13	DTrp	Orn	(pCN)Phe	7.92 ± 0.07	na	0.0	8.15 ± 0.05
14	Trp	Lys	(pNO_2)Phe	8.75 ± 0.05	9.20 ± 0.08[j]	95 ± 20	nd
15	DTrp	Orn	(pNO_2)Phe	7.77 ± 0.08	na	0.0	8.12 ± 0.07

[a]Cys in *h*U-II and *h*U-II(4−11). [b]Binding assay with recombinant human UT receptor and radioligand [^{125}I]urotensin-II pK_i: −log K_i. [c]Contractile activity in a rat aorta bioassay, pEC_{50}: −log EC_{50}. [d]Percent versus *h*U-II. [e]pK_B: log(CR − 1) − log [B]. Each value in the table is mean ± SEM of at least three or four determinations. [f]For hU-II, N-terminus = H-Glu-Thr-Pro-Asp. [g]For the structure of unconventional amino acids, see Figure 1. [h]$p < 0.05$ vs hU-II E_{max} (two-tail Student's *t*-test for paired data). [i]$p < 0.05$ vs **1** (ANOVA and Dunnett's post hoc test). [j]$p < 0.05$ vs hU-II (two-tail Student's *t*-test for paired data); na, not active; nd, not determinable.

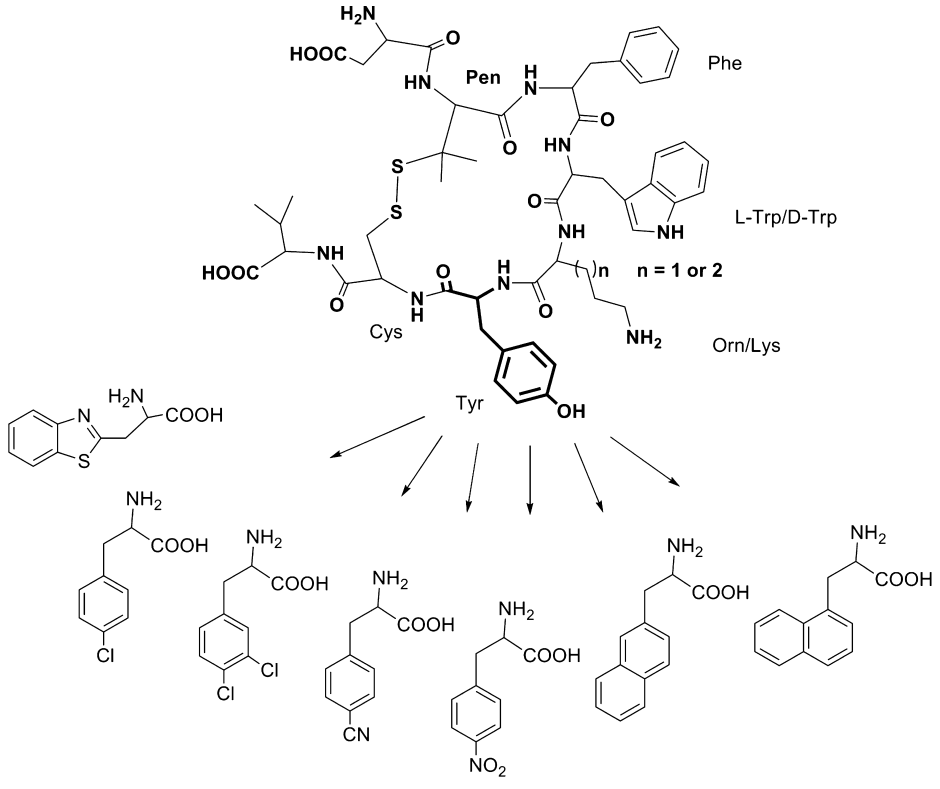

Figure 1. General view of synthesized compounds.

Hence, most of the peptides developed to date have been constructed on the basis of this sequence.[20−24]

Previously, we have identified two important analogues of *h*U-II(4−11), specifically, the superagonist **1** (P5U), H-Asp-c[Pen-Phe-Trp-Lys-Tyr-Cys]-Val-OH,[25] and the antagonist urantide, H-Asp-c[Pen-Phe-DTrp-Orn-Tyr-Cys]-Val-OH[26] (Table 1), which are nowadays recognized as the most potent peptide ligands at the UT receptor so far described. Interestingly, urantide has been extensively used not only as a valid tool to investigate the urotensinergic system role, but it has also been recently ascertained that urantide can protect against atherosclerosis in rats.[27]

dx.doi.org/10.1021/jm500218x | J. Med. Chem. XXXX, XXX, XXX−XXX

As part of our ongoing effort to improve the potency and stability of urotensin-II analogues,[28,29] in this study, we have designed and synthesized novel analogues of **1** and urantide by the exchange of Tyr^9 residue with aromatic noncoded amino acids (Figure 1). We found novel analogues with improved agonist activity compared to the parent **1** and antagonist peptides alike urantide.[30] Also, these new ligands showed good stability in the serum proteolytic assay, a key factor in enhancing the bioavailability of peptides. These analogues allowed us to improve the knowledge about the structure− and conformation−activity relationships related to U-II peptide derivatives and represent valid means to better investigate the importance of U-II in physio/pathological conditions.

RESULTS

Design. A SAR study on Tyr^9 was prompted by our recent finding that the side chain orientation of this residue influences the activity of **1** and urantide constrained analogues.[31] Hence, we replaced Tyr with aromatic noncoded amino acids (Figure 1). Noncoded amino acids were chosen in an attempt to improve the serum stability. We started with bulky electron-rich aromatic moieties in compounds **2**−**7** or phenyl ring substituted with bulky chlorine atoms (**8**−**11**). Alternatively, the electron-donating hydroxyl group of Tyr^9 was replaced by electron-withdrawing groups such as cyano (**12**, **13**) or nitro (**14**, **15**). Peptides were synthesized and analyzed as reported in the Experimental Section and Supporting Information (Tables S1 and S2).

Biological Data. Sequences, receptor binding affinity at *h*-UT, and biological activity (rat aorta bioassay) of the designed compounds are reported in Table 1. To evaluate the suitable features of the aromatic residue in position 9 and, in particular, the contribution of the phenolic group, we replaced Tyr^9 with several aromatic uncoded amino acids (Figure 1), in both sequences of **1** and urantide (compounds **2**−**15**). First, we used amino acids with a bulkier aromatic group, that is, (1)Nal, (2)Nal, and Btz. The substitution of the native Tyr^9 residue in **1** by a (2)Nal residue (compound **2**) generated an analogue of similar contractile potency (pEC_{50} = 9.14 ± 0.06, Figure S1, Supporting Information) and a reduced binding affinity of 1 log unity (pK_i = 8.70 ± 0.08). Similar modification in urantide sequence produced compound **3** with improved binding affinity when compared to urantide (pK_i = 9.14 ± 0.08). Anyway, this compound retains a small residual agonist activity (E_{max} = 13 ± 5%). Compound **4** [(1)Nal/Tyr replacement in **1**] was shown to be a less potent agonist than **1** (pEC_{50} = 8.3 ± 0.2, E_{max} = 86 ± 5%), although it showed good receptor affinity (pK_i = 9.40). The same substitution [(1)Nal/Tyr replacement] was introduced in the urantide sequence to give compound **5** with a partial agonist activity (pEC_{50} = 7.74 ± 0.10, E_{max} = 37 ± 9%). In compound **6** (UPG-100),[30] we replaced Tyr^9 with a residue of benzothiazolylalanine (Btz), an analogue of Trp in which the indole group is replaced by a benzothiazolyl moiety, which is a highly electron-rich system. Compound **6** was shown to be a significantly (p < 0.05) more potent agonist compared to **1** (pEC_{50} = 10.71 ± 0.04, E_{max} = 89 ± 16%). In parallel, compound **7** (Btz^9 derivative of urantide) showed an increased partial agonist activity (E_{max} = 57 ± 2%) compared to analogues **3** and **5**.

Then, Tyr^9 residue was replaced with some aromatic amino acids containing an isoster of phenolic group in the para position. Replacing the Tyr^9 residue in **1** with the amino acid (pCl)Phe led to a compound with similar activity to the parent peptide. In fact, compound **8** showed a comparable potency in the functionality assay (pEC_{50} = 9.09 ± 0.12, E_{max} = 85 ± 10%) albeit with a slight reduction in binding affinity at the UT receptor (pK_i = 8.91 ± 0.07). Instead, compound **9** resulted in a weak partial agonist (E_{max} = 13 ± 3%) with an improved binding affinity profile (pK_i = 8.98 ± 0.05).

Interestingly, replacing the Tyr^9 residue with the amino acid (3,4-Cl)Phe generated compound **10** (UPG-92)[30] with a high agonist activity (pEC_{50} = 10.9 ± 0.14, p < 0.05 compared to **1**; E_{max} = 102 ± 8%), resulting it a superagonist. As expected, this compound is about 1.6 log more potent than **1** and represents the most potent peptide agonist at the UT receptor discovered to date. Compound **11**, the (3,4-Cl)Phe^9 derivative of urantide, similarly to compound **9**, resulted in a partial agonist with increased efficacy compared to the last (E_{max} = 26 ± 7 vs 13 ± 3%).

The phenolic OH group was then replaced by electron-withdrawing groups in compounds **12**−**15**. Compound **12**, in which Tyr^9 was replaced with a (pCN)Phe residue, was less potent as an agonist compared to **1** (pEC_{50} = 8.97, E_{max} = 79 ± 1) and with a reduced binding affinity (pK_i = 8.74 ± 0.10). Interestingly, compound **13** (UPG-83),[30] the (pCN)Phe^9 derivative of urantide, showed behavior as an antagonist, producing a parallel rightward shift (Figure S2, panel A, Supporting Information) of the agonist response curves without depressing the agonist E_{max}. Schild-plot analysis was consistent with competitive antagonism [slope = 0.918, 95% confidence level (cl) = 0.758−1.080], and a pK_B value of 8.15 ± 0.05 was calculated (Figure S2, panel B, Supporting Information), comparable to that of urantide (Table 1). Finally, replacing the Tyr^9 residue with the amino acid (pNO_2)Phe led to compounds with similar activity compared to the respective parent peptides. In fact, compound **14** was shown to have agonist activity comparable to that of **1** (pK_i = 8.75 ± 0.05, pEC_{50} = 9.20 ± 0.08, E_{max} = 95 ± 20%), and compound **15** (UPG-95)[30] revealed behavior as an antagonist comparable to that of urantide, producing a parallel rightward shift of the agonist response curves. Also for this compound Schild-plot analysis was consistent with competitive antagonism (slope = 0.900, 95% cl = 0.660−1.140) and a pK_B value of 8.12 ± 0.07 was calculated (Figure S2, panels C and D, Supporting Information) (Table 1). The ability of the newly discovered antagonist analogues to stimulate calcium mobilization like urantide was also evaluated. Both peptides **13** and **15** behave as partial agonists in this assay, showing an increased efficacy compared to that of urantide. The intracellular calcium assay was performed according to the manufacturer's protocol (DiscoveRx Corp., Fremont, CA) described in the Experimental Section. Results are reported in Table 2.

Peptides Stability. To investigate the effects of the modifications of peptides on proteolytic susceptibility, the

Table 2. Intracellular Calcium Efficacy

	Ca^{2+} efflux efficacy (%)[a]	
compd	1 μM	10 μM
urantide	43.3 ± 0.8	46.2 ± 0.6
13	61.4 ± 1.5[b]	61.7 ± 3.3
15	56.5 ± 0.2[b]	61.2 ± 3.8

[a]Efficacy is expressed as percent of the maximum response to *h*U-II. Each value in the table is the mean ± SEM of three determinations. [b]p < 0.05 vs the respective value of urantide (ANOVA and Dunnett's post hoc test).

dx.doi.org/10.1021/jm500218x | J. Med. Chem. XXXX, XXX, XXX−XXX

disappearance of the intact peptides incubated in diluted serum at 37 °C was followed by RP-HPLC (Supporting Information, Figure S3);[32] peptides *h*U-II(4−11), urantide, **1**, **10**, and **13** were assayed. Overall results, shown in Figure 2, display the course of

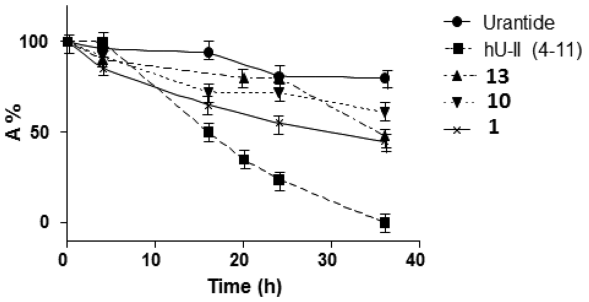

Figure 2. Resistance to enzyme degradation of *h*U-II(4−11), urantide, **1**, **10**, and **13** was assessed by incubation in 25% FCS for 36 h. Residual peptide quantity, expressed as the percentage of the initial amount versus time (h), was plotted. The results represent the average of three independent experiments.

degradation up to 36 h to highlight the differences in the profiles of the degraded peptides. After 16 h of treatment, *h*U-II(4−11) had a residual concentration lower than 50% and for **1** it was about 65%, while for other compounds it was higher than 70% of the initial concentration. After 36 h, compound **10** showed a residual concentration higher than 50%, while for **1** the concentration was slightly lower (about 45%). Clearly, developed peptides are very stable in 25% FCS.

NMR Analysis. A whole set of 1D and 2D NMR spectra in 200 mM aqueous solution of SDS was collected for compounds **10** and **13**. These peptides were chosen since compound **10** behaves as a superagonist compared to **1**, while compound **13** is a potent antagonist devoid of agonist activity in the rat aorta assay (Table 1). SDS micelle solutions were used, since they are membrane mimetic environments and are largely used for conformational studies of peptide hormones and antimicrobial peptides.[33−36]

Complete ^{1}H NMR chemical shift assignments were effectively achieved for the two peptides according to the Wüthrich[37] procedure via the usual systematic application of DQF-COSY, TOCSY, and NOESY experiments with the support of the XEASY software package (Supporting Information, Tables S3 and S4). Peptide **10** differs from **1** only for the (3,4-Cl)Phe/Tyr^{9} substitution, and peptide **13** differs from urantide only for the (pCN)Phe/Tyr^{9} substitution. Indeed, they show diagnostic NMR parameters (H_α proton chemical shifts, NOE contacts, and $^{3}J_{NH\text{-}H\alpha}$ coupling constants, NH exchange rates, and temperature coefficients) all similar to those observed in the corresponding parent peptides (Supporting Information, Tables S3−S6). In particular, NOE contacts between H_α−NH_{i+2} of (D)Trp^{7} and residue 9 and between NH−NH_{i+1} of Lys(Orn)^{8}

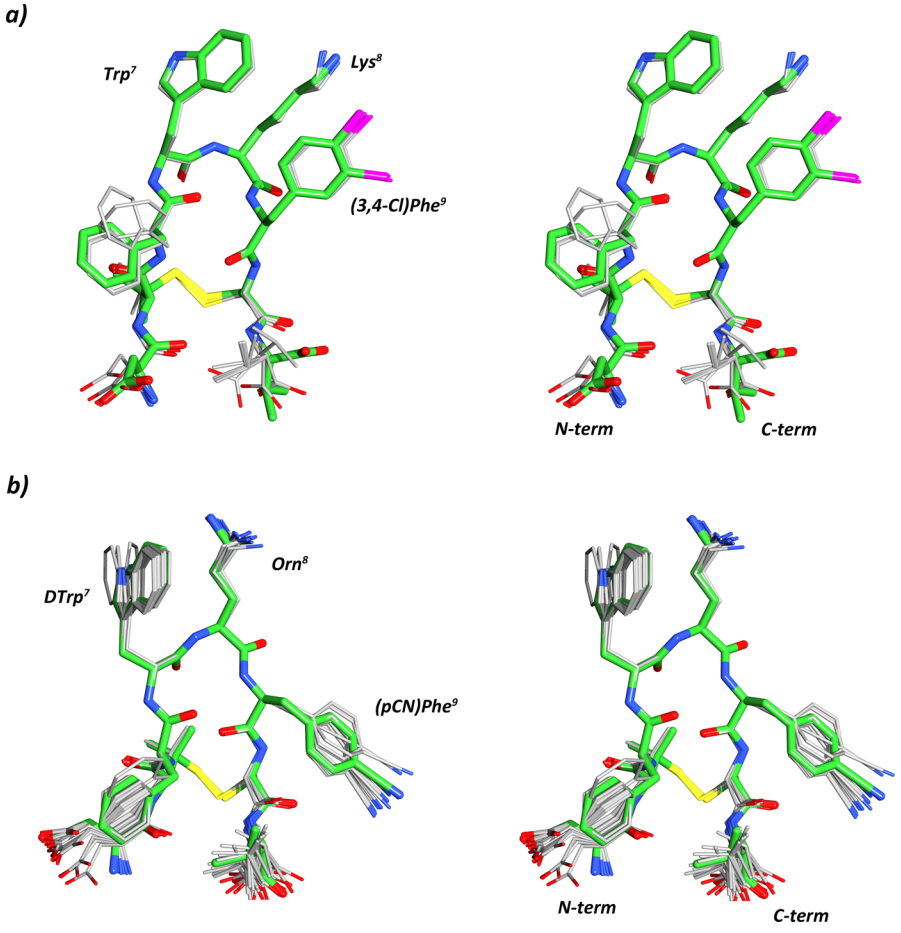

Figure 3. Stereoview of the superposition of the 10 lowest energy conformers of **10** (a) and **13** (b). Structures were superimposed using the backbone heavy atoms of residues 5−10. Heavy atoms are shown with different colors (carbon, green; nitrogen, blue; oxygen, red; sulfur, yellow; chlorine, magenta). Hydrogen atoms are not shown for clarity.

dx.doi.org/10.1021/jm500218x | *J. Med. Chem.* XXXX, XXX, XXX−XXX

and residue 9 indicated the presence of a β-turn. This result was supported by the observation of a slowly exchanging NH resonance of residue 9 and the low value of the temperature coefficient for this proton ($-\Delta\delta/\Delta T$ < 3.0 ppb/K). A short stretch of antiparallel β-sheet involving residues 5−6 and 10−11 is inferred from a number of long-range NOEs, including H_α−NH connectivities between residues 5, 11 and 10, 6 and a NH−NH connectivity between residues 6 and 9. All the data indicated the preservation, in **10** and **13**, of the β-hairpin structure. As for the parent peptides, a number of NOE interactions connect (D)Trp^7 with Lys(Orn)^8 side chains, indicating a close proximity between them (Supporting Information, Figures S4 and S5). (3,4-Cl)Phe side chain of peptide **10** shows NOE contacts with Lys^8 (Supporting Information, Figure S4). In contrast, (pCN)-Phe^9 of peptide **13** has intense NOE contacts with the Val^{11} side chain and only a weak NOE with Orn^8 Hγ's (Supporting Information, Figure S5). These results point to a different orientation of residue 9 side chain in the two peptides. NMR-derived constraints obtained for the analyzed peptides (Supporting Information, Tables S5 and S6) were used as the input data for a simulated annealing structure calculation. For each peptide, 20 calculated structures satisfying the NMR-derived constraints (violations smaller than 0.20 Å) were chosen (Figure 3a,b). As shown, both peptides **10** and **13** show a well-defined type II′ β-hairpin structure encompassing residues 5−10 (backbone rmsd values are 0.36 and 0.27 Å, respectively). In contrast, the N- and C-terminal residues were more flexible.

Considering the orientation of the side chains, Phe^6, (D)Trp^7, and Orn^8 χ_1 angles showed a large preference for trans, trans, and g^- rotamers, respectively. In urantide, the dihedral angle χ_2 of DTrp^7 was about 125° or −70°, in accordance with strong NOEs between H_α and $H_{\varepsilon 3}$ or $H_{\delta 1}$, respectively (Supporting Information, Table S6). Finally, the side chain of residue 9 is found to be preferentially in the g^- and trans orientation in peptides **10** and **13**, respectively.

DISCUSSION

As part of our ongoing efforts to improve the potency and stability of urotensin analogues discovered previously in our laboratories and the knowledge about their SARs, we have designed and synthesized a series of analogues of **1** and urantide in which the Tyr^9 residue was replaced with aromatic noncoded amino acids (Table 1). Tyr^9 belongs to the WKY pharmacophoric sequence of U-II, which is crucial for interaction with its receptor, as demonstrated by previous studies. In fact, the replacement of W, K, and Y induces large changes in biological activity, suggesting the importance of the side chains of these residues for binding to and activating the UT receptor.[20−22,38] In this study the phenol moiety of **1** and urantide was replaced with bulky electron-rich aromatic moieties in compounds **2**−**7** or a phenyl ring substituted with bulky chlorine atoms (**8**−**11**). Alternatively, the electron-donating hydroxyl group of the Tyr^9 was replaced by electron-withdrawing groups such as cyano (**12**, **13**) or nitro (**14**, **15**). All synthesized compounds were tested for their binding affinity on *h*-UT-transfected CHO cells and for their contractile activity on de-endothelialized rat aortic rings (Table 1).[26] Overall, bioactivity results (Table 1) indicate that in the **1** derivatives the substitution of Tyr^9 with other aromatic-based moieties is well-tolerated. In fact, all these compounds gave a rat aorta contraction of at least 70%. These SARs are in accordance with previous results,[19,21] which demonstrated that Tyr^9 in *h*U-II or *h*U-II(4−11) can be replaced by various aromatic residues with preservation of most of the agonist activity, at least when the flexibility of the Tyr^9 side chain is kept.[39] The best results for the **1** derivatives were obtained by replacing tyrosine by bulky Btz (**6**) or (3,4-Cl)Phe (**10**) residues, significantly improving in both cases the potency by more than one log (pEC_{50} = 10.71 and 10.9, respectively, p < 0.05 vs **1**) compared to **1** (pEC_{50} = 9.4 ± 0.2) and more than two logs compared to the endogenous agonist *h*U-II (pEC_{50} = 8.50 ± 0.06). Note that peptide **10** is the most potent UT agonist discovered to date. We and others[21,28] have shown that bulky aromatic amino acids may increase the binding affinity and the biological activity of the U-II agonists through an enhancement of the hydrophobic interactions within a putative Tyr binding pocket of UT.

To the best of our knowledge the SAR studies on position 9 of urantide derivatives are unprecedented. Like **1**, urantide seems also to tolerate aromatic substitutions at position 9; as a matter of fact, all derivatives bind to UT receptor with $pK_i \geq 7.77$. The main result obtained in this series is the finding of two antagonists, compounds **13** and **15**. Despite a slight loss of affinity, these compounds behave as pure antagonists in the rat aorta bioassay, like the parent urantide. SAR data clearly indicate that small polar groups (pCN, pNO_2, and the original OH) are required for pure antagonist activity. In contrast, bulky lipophilic moieties [(1)Nal, (3,4-Cl)Phe, Btz] increase the agonist activity (efficacy) of urantide derivatives.

As widely discussed elsewhere,[34] urantide behaves as a partial agonist in a calcium mobilization assay performed in CHO cells expressing the *h*-UT.[40] The same behavior was shown by compounds **13** and **15**, i.e., pure antagonist in the aorta assay and partial agonist in a calcium mobilization assay, although with slightly higher efficacy compared to urantide (Table 2). Nevertheless, it is well-known that urantide has been used by several groups as reference antagonist compound in studies of the urotensinergic system.[27,41] These novel ligands can be useful to discriminate the partial agonism/antagonism effects at the UT receptor in different cell lines/tissues. Also, the availability of novel agonists and antagonists as pharmacological tools to investigate the urotensinergic system is very important, since subtle pharmacokinetic differences can differentiate their effects in vivo. In this respect, stability tests were performed on peptide *h*U-II(4−11), **1**, urantide, and derivatives **10** and **13**. These studies demonstrated that urantide and peptides **10** and **13** are highly stable, showing a residual concentration higher than 50% in fetal calf serum even after 36 h (Figure 2). The higher level of stability shown by urantide, **1**, **10**, and **13** compared to *h*U-II may be tentatively ascribed to the presence of a Pen residue, which can hinder the reduction of the disulfide bridge. The effect on serum stability of aromatic noncoded amino acid is variable, with **10** being more stable than **1**, while **13** is less stable than urantide.

A conformational analysis by solution NMR of the most interesting derivatives **10** and **13** was also carried out. In previous works,[33,34] we showed that *h*U-II analogues, which retain high affinity for the UT receptor, all possess a type II′ β-hairpin backbone conformation, regardless their agonist or antagonist activity, indicating that such backbone conformation is necessary for the UT recognition. Indeed, such backbone conformation is observed also in the novel derivatives (Figure 3) confirming the above outcome. The main conformational difference observed in the structures of peptides **10** (agonist activity) and **13** (antagonist activity) is established in a different orientation of the (3,4-Cl)Phe or (pCN)Phe side chain, respectively. In particular, while in the agonist **10** the (3,4-Cl)Phe^9 is close to the Lys^8 side chain (Figures 3a and S4, Supporting Information),

dx.doi.org/10.1021/jm500218x | J. Med. Chem. XXXX, XXX, XXX−XXX

in the antagonist **13**, the (pCN)Phe[9] side chain is close to the Val[11] side chain and far from the Orn[8] side chain (Figures 3b and S5, Supporting Information). This result is in accordance with the one obtained by studying constrained analogues of **1** and urantide[31] and with a revision of the conformational preferences of urantide performed using DPC micelles.[42] In particular, in our first work,[31] we demonstrated that while the orientation of the Trp[7] indole moiety is irrelevant for the agonist/antagonist activity switching, the Tyr[9] phenol orientation influences peptide activity. Note that the signal spread of the ^{1}H NMR resonances of both **10** and **13** is better than that observed in the spectra of the published *h*U-II analogues with less overlapping, which led to a higher number of experimental constraints and structure reliability.

CONCLUSIONS

In this work, analogues of **1** and urantide modified at the Tyr[9] position were developed. Two of them, compounds **6** and **10**, showed increased potency compared to the parent superagonist peptide **1**. Two urantide analogues, compounds **13** and **15**, turned out to be pure antagonists in the rat aorta bioassay, like parent urantide. Compounds **10** and **13** showed also a good stability in the serum proteolytic assay, suggesting that these peptides may be stable enough to give them an additional opportunity in drug delivery. Furthermore, these novel analogues allowed us to improve the knowledge on structure− and conformation−activity relationships on UT receptor ligands, which can help in the design of improved compounds.

Ultimately, these novel ligands, such as the superagonist **10**, which is the most potent agonist discovered to date, could be useful pharmacological tools for in vitro and in particular in vivo studies aimed at clarifying the role played by the U-II/UT system in physiopathological conditions.

EXPERIMENTAL SECTION

Chemistry. N^{α}-Fmoc-protected amino acids, HBTU, and HOBt were purchased from Inbios (Naples, Italy). Wang resin was purchased from Advanced ChemTech (Louisville, KY). Protected Pen was purchased from Bachem (Basel, Switzerland). Peptide synthesis solvents and reagents, as well as CH_3CN for HPLC, were reagent grade and were acquired from commercial sources and used without further purification unless otherwise noted. All synthesized compounds showed a purity >98%, as determined by analytical RP-HPLC.

Materials for NMR. ^2H_2O (99.9%) was obtained from Aldrich (Milwaukee, WI), 98% SDS-d_{25} was obtained from Cambridge Isotope Laboratories, Inc. (Andover, MA), and [(2,2,3,3-tetradeuterio-3-(trimethylsilanyl)]propionic acid (TSP) was from MSD Isotopes (Montreal, Canada).

Synthesis. The synthesis of *h*U-II analogues was performed in a stepwise fashion via the solid-phase method.[43] The first amino acid, N^{α}-Fmoc-Val-OH, was coupled to Wang resin (0.5 g, 0.7 mmol of NH_2/g) in the presence of DMAP.[44] The following protected amino acids were then added stepwise: N^{α}-Fmoc-Cys(Trt)-OH, N^{α}-Fmoc-R-OH [R = Nal(1), Nal(2), Btz, (pCl)Phe, (3,4-Cl)Phe, (pCN)Phe, (pNO_2)Phe], N^{α}-Fmoc-Yaa($N^{\varepsilon/\delta}$-Boc)-OH (Yaa: Lys, Orn), N^{α}-Fmoc-Xaa(N^{in}-Boc)-OH (Xaa: Trp, DTrp), N^{α}-Fmoc-Phe-OH, N^{α}-Fmoc-Pen(Trt)-OH, and N^{α}-Fmoc-Asp(OtBu)-OH. Each coupling reaction was accomplished using a 3-fold excess of amino acid with HBTU and HOBt in the presence of DIEA.

The N^{α}-Fmoc protecting groups were removed by treating the protected peptide resin with a 25% solution of piperidine in DMF (1 × 5 min and 1 × 20 min). The peptide resin was washed three times with DMF, and the next coupling step was initiated in a stepwise manner. All reactions were performed under an Ar atmosphere. The peptide resin was washed with DCM (3×), DMF (3×), and DCM (4×), and the deprotection protocol was repeated after each coupling step. The N-terminal Fmoc group was removed as described above, and the peptide was released from the resin with TFA/Et_3SiH/H_2O 90:5:5 for 3 h. The resin was removed by filtration and the crude peptide was recovered by precipitation with cold anhydrous ethyl ether to give a white powder which was purified by RP-HPLC on a semipreparative C18-bonded silica column (Phenomenex, Jupiter 4 μ Proteo 90 Å, 1.0 × 25 cm) using a gradient of CH_3CN in 0.1% aqueous TFA (from 10 to 90% in 40 min) at a flow rate of 5.0 mL/min. The product was obtained by lyophilization of the appropriate fractions after removal of the CH_3CN by rotary evaporation. Analytical RP-HPLC indicated for all synthesized compounds a purity >98%, and the correct molecular weights were confirmed by LC/ESI-MS (6110 Quadrupole, Agilent Technologies). The quantitative amino acid analysis was performed using an Applied Biosystems model 420A (Table S2, Supporting Information).

General Method of Oxidation and Cyclization. The peptides were oxidized by the syringe pump method previously reported.[45] The linear peptide (300−500 mg) was dissolved in 40 mL of H_2O/acetonitrile/methanol 2:1:1, and nitrogen gas was passed through the solution for 20 min. Five milliliters of saturated ammonium acetate solution was added, and the pH was taken to 8.5 with NH_4OH. The peptide solution was then added at room temperature via syringe pump to a stirred oxidant solution. The oxidant solution was prepared as follows: 2 equiv of potassium ferricyanide was dissolved in 800 mL of H_2O/acetonitrile/methanol 2:1:1. To this solution was added 100 mL of saturated ammonium acetate, and the pH was then taken to 8.5 with NH_4OH. The peptide solution was added at such a rate that approximately 10 mg of peptide was delivered per hour per liter of the oxidant. After the addition of peptide was complete, the reaction mixture was stirred for an additional 5−6 h and then taken to pH 3.5 with glacial acetic acid. Amberlite IRA-68 (Cl^- form) was added to remove the iron ions, and the solution was stirred for 20 min and then filtered. The solution was concentrated using a rotary evaporator at 30 °C and then lyophilized. The material thus obtained was dissolved in glacial acetic acid, filtered to remove inorganic salts, and relyophilized. The crude cyclic peptides were purified by preparative HPLC on the system described above, using a gradient of 0.1% aqueous TFA for 20 min and then 0−20% acetonitrile in 5 min, followed by 20−60% acetonitrile in 40 min, all at 5 mL/min. Again the peptides eluted near organic/0.1% aqueous TFA 1:1. The purity of the cyclic peptides was checked by analytical HPLC (Phenomenex Luna 5 μ, 100 Å, 150 × 4.6 mm), using a Shimadzu SPD 10AVP with detection at 230 and 254 nm and by TLC in four solvent systems in silica gel with detection by UV light, iodine vapors, and ninhydrin. The analytical data of the compounds synthesized in this paper are given in the Supporting Information.

Organ Bath Experiments. The experimental procedures employed in this study were approved by the Institutional Animal Care and Use Committee and carried out in accordance with the legislation of Italian authorities (D.L. 116 27/01/1992), which complies with European Community guidelines (CEE Directive 86/609) for the care and use of experimental animals.

Male albino rats (Wistar strain, 275−350 g; Harlan Laboratories) were euthanized by cervical dislocation, under ether anesthesia. The thoracic aorta was cleared of surrounding tissue and excised from the aortic arch to the diaphragm. From each vessel, a helically cut strip was prepared, and then it was cut into two parallel strips. The endothelium was removed by gently rubbing the vessel intimal surface with a cotton-tipped applicator; the effectiveness of this maneuver was assessed by the loss of relaxation response to acetylcholine (1 μM) in noradrenaline (1 μM) precontracted preparations. All preparations were placed in 5 mL organ baths filled with normal Krebs solution of the following composition (mmol/L): NaCl, 119; $NaHCO_3$, 25; KH_2PO_4, 1.2; $MgSO_4$, 1.5; $CaCl_2$, 2.5; KCl, 4.7; and glucose, 11. The Krebs solution was warmed at 37 °C and oxygenated with 95% O_2, 5% CO_2. The tissues were connected to isotonic force transducers (Ugo Basile) under a constant load of 5 mN, and motor activity was digitally recorded by an Octal bridge amplifier connected to PowerLab/8sp hardware system and analyzed using the Chart 4.2 software (ADInstruments Ltd., Oxford, UK). After 60 min equilibration, tissue responsiveness was assessed by

dx.doi.org/10.1021/jm500218x | J. Med. Chem. XXXX, XXX, XXX−XXX

the addition of 1 μM noradrenaline followed by a further equilibration of 60 min.

To assess the agonist activity, cumulative concentration−response curves of *h*U-II and the agonist peptide under examination were constructed in paired aortic strips, and responses obtained were normalized toward the control *h*U-II maximal contractile effect (E_{max}).

To assess the antagonist activity, concentration−response curves of *h*U-II were constructed cumulatively in paired aortic strips. One strip was pretreated with vehicle (DMSO; 1−3 μL/mL) and used as a control, while the other strip was pretreated with the antagonist peptide under examination, and after a 30 min incubation period, *h*U-II was administered cumulatively to both preparations.

In each preparation only one cumulative concentration−response curve of *h*U-II was carried out, and only one concentration of antagonist was tested. Concentration−response curves were analyzed by sigmoidal nonlinear regression fit using the GraphPad Prism 4.0 program (San Diego, CA) to determine the molar concentration of the agonist producing the 50% (EC_{50}) of its maximal effect. The agonist activity of all compounds was expressed as pEC_{50} (−log EC_{50}). The antagonist potency was expressed in terms of pK_B estimated as the mean of the individual values obtained with the Gaddum equation: $pK_B = \log(CR - 1) - \log [B]$ were CR is the concentration ratio calculated from equieffective concentrations of agonist (EC_{50}) obtained in the presence and in the absence of antagonist and B is the antagonist concentration used.[46] Competitive antagonism was checked by the Schild regression analysis by plotting the estimates of $\log(CR - 1)$ against $\log [B]$ to determine the slopes of linear regression; a plot with linear regression line and slope not significantly different from unity was considered as proof of competitive antagonism.[46]

Results were compared for significant differences using the two-tail Student's *t* test for paired data or one-way analysis of variance (ANOVA) followed by Dunnett's post hoc test. A p value <0.05 was considered statistically significant.

Binding Experiments. All experiments were performed on membranes obtained from stable CHO-K1 cells expressing the recombinant human UT receptor (ES-440-M, lots 564-915-A and 613-577-A, PerkinElmer, Boston, MA). Assay conditions were Tris buffer (20 mM, pH 7.4 at 37 °C) added with $MgCl_2$ (5 mM) and 0.5% BSA. The final assay volume was 0.1 mL, containing 1 or 20 μg membrane proteins depending on the lot of provided membranes. The radioligand used for competition experiments was [^{125}I]urotensin II (specific activity 2200 Ci/mmol; NEX379, PerkinElmer) in the range 0.07−1.4 nM (as recommended by the lot of provided membranes). Nonspecific binding was determined in the presence of 1 μM of unlabeled *h*U-II and ranged between 10 and 20% of the total binding. Competing ligands were tested in a wide range of concentrations (1 pM to 10 μM). The incubation period (120 min at 37 °C) was terminated by rapid filtration through UniFilter-96 plates (Packard Instrument Co.), presoaked for at least 2 h in BSA 0.5%, and using a MicroMate 96 cell harvester (Packard Instrument Co.). The filters were then washed four times with 0.2 mL aliquots of Tris-HCl buffer (20 mM, pH 7.4, 4 °C). Filters were dried and soaked in Microscint 40 (50 μL in each well, Packard Instrument Co.), and bound radioactivity was counted by a TopCount microplate scintillation counter (Packard Instrument Co.). Determinations were performed in duplicate. All binding data were fitted by using GraphPad Prism 4.0 in order to determine the equilibrium dissociation constant (K_d) from homologous competition experiments and the ligand concentration inhibiting the radioligand binding of the 50% (IC_{50}) from heterologous competition experiments. K_i values were calculated from IC_{50} using the Cheng−Prusoff equation ($K_i = IC_{50}/(1 + [\text{radioligand}]/K_d)$) according to the concentration and K_d of the radioligand.[45] In each experiment, one homologous competition curve of urotensin-II was run, and the calculated K_d and the used radioligand concentration were used for the determination of ligand K_i values. The determine K_d value was 2.23 nM (1.09−3.38 nM, 95% cl, n = 5, each experiment performed in duplicate).

Intracellular Calcium Assay. The intracellular calcium assay was performed by DiscoveRx (Fremont, CA) using a HitHunter Calcium No WashPLUS assay kit from DiscoveRx Inc. (Fremont, CA), and UT-CHO-K1 cells were transfected with the cDNA encoding UT-II human receptor.

Twenty-four hours prior to assay, cells were seeded at 10 000 cells per well of a 384-well plate (Greiner, black optical poly-D-lysine coated) in 20 μL of cell plating reagent 2 (DiscoveRx) and incubated overnight at 37 °C. Cells were loaded with a Calcium No WashPLUS kit (DiscoveRx) for 45 min at 37 °C + 15 min at room temperature in the presence of probenecid (5 mM).[47] Compound addition and calcium mobilization were monitored on a FLIPR^{TETRA} (Molecular Devices, Sunnyvale, CA).

Serum Peptides Stability. Peptide stabilities were assayed in diluted serum as previously described.[48] Fetal calf serum (25%) was centrifuged at 13 000 rpm for 10 min to remove lipids, and the supernatant was collected and incubated at 37 °C for at least 15 min. The assay was initiated upon the addition of peptides to the serum for a final peptide concentration of 80 μM, and 80 μL aliquots of the incubations were taken at the following time points: 0, 4, 16, 20, 24, and 36 h. The aliquots were mixed with 40 μL of 15% trichloroacetic acid (TCA) and incubated at 2 °C for at least 15 min to precipitate serum proteins.

The supernatant was collected for each sample after centrifugation at 13 000 rpm for 10 min. These assays were performed in triplicate. Reverse-phase high-performance liquid chromatography (RP-HPLC) was carried out on an Agilent Technologies 1200 series HPLC equipped with UV detector using a C18 column from ThermoFisher (Milan, Italy). Gradient elution was performed at 25 °C (monitoring at 210 nm) in a gradient starting with buffer A (0.1% TFA in water) and applying buffer B (0.1% TFA in acetonitrile) from 5 to 70% in 15 min (Supporting Information, Figure S3).

NMR Spectroscopy. The samples for NMR spectroscopy were prepared by dissolving the appropriate amount of peptide in 0.45 mL of ^1H_2O (pH 5.5), 0.05 mL of ^2H_2O to obtain a concentration 1−2 mM of peptides, and 200 mM of SDS-d_{25}. NH exchange studies were performed by dissolving peptides in 0.50 mL of ^2H_2O and 200 mM of SDS-d_{25}. NMR spectra were recorded on a Varian INOVA 700 MHz spectrometer equipped with a *z*-gradient 5 mm triple-resonance probe head. All the spectra were recorded at a temperature of 25 °C. The spectra were calibrated relative to TSP (0.00 ppm) as internal standard. One-dimensional (1D) NMR spectra were recorded in the Fourier mode with quadrature detection. The water signal was suppressed by gradient echo.[49] 2D DQF-COSY,[50] TOCSY,[51] and NOESY[52] spectra were recorded in the phase-sensitive mode using the method of States et al.[53] Data block sizes were 2048 addresses in t_2 and 512 equidistant t_1 values. Before Fourier transformation, the time domain data matrices were multiplied by shifted $\sin^2$ functions in both dimensions. A mixing time of 70 ms was used for the TOCSY experiments. NOESY experiments were run with mixing times in the range of 150−300 ms. The qualitative and quantitative analyses of DQF-COSY, TOCSY, and NOESY spectra were obtained using the interactive program package XEASY.[54] $^3J_{HN\text{-}H\alpha}$ coupling constants were obtained from 1D ^{1}H NMR and 2D DQF-COSY spectra. The temperature coefficients of the amide proton chemical shifts were calculated from 1D ^{1}H NMR and 2D TOCSY experiments performed at different temperatures in the range 25−40 °C by means of linear regression.

Structural Determinations. The NOE-based distance restraints were obtained from NOESY spectra collected with a mixing time of 200 ms. The NOE cross-peaks were integrated with the XEASY program and were converted into upper distance bounds using the CALIBA program incorporated into the program package DYANA.[55] Cross-peaks which were overlapped more than 50% were treated as weak restraints in the DYANA calculation. In a first step only NOE-derived constraints (Supporting Information) were considered in the annealing procedures. For each examined peptide, an ensemble of 200 structures was generated with the simulated annealing of the program DYANA. An error-tolerant target function (tf-type = 3) was used to account for the peptide intrinsic flexibility. Nonstandard Pen, DTrp, Orn, (pCN)Phe, and (3,4-Cl)Phe residues were added to DYANA residue library using MOLMOL.[56] From these structures we could univocally determine the hydrogen bond atom acceptors corresponding to the slowly exchanging NH's previously determined for each peptide. In a second DYANA run, these hydrogen bonds were explicitly added as upper and lower limit

dx.doi.org/10.1021/jm500218x | J. Med. Chem. XXXX, XXX, XXX−XXX

constraints (NH of Phe[6] with CO of Xaa[9], and NH of Xaa[9] with CO of Phe[6]), together with the NOE-derived upper limit constraints (Supporting Information). The second annealing procedure produced 200 conformations from which 50 structures were chosen, the interprotonic distances of which best fitted NOE-derived distances. The confirmations were then refined through successive steps of restrained and unrestrained EM calculations using the Discover algorithm (Accelrys, San Diego, CA) and the consistent valence force field (CVFF)[57] as previously described.[33] The final structures were analyzed using the InsightII program (Accelrys, San Diego, CA). Graphical representation was carried out with the InsightII program (Accelrys, San Diego, CA). RMS deviation analysis between energy-minimized structures was carried out with the program MOLMOL.[56]

■ ASSOCIATED CONTENT

Ⓢ Supporting Information

Analytical data of the synthesized peptides, functional activity profiles, NMR data of the analyzed peptides, and details on serum stability tests. This material is available free of charge via the Internet at http://pubs.acs.org.

■ AUTHOR INFORMATION

Corresponding Author

*Phone: +39-081-678620. Fax: +39-081-678644. E-mail: paolo.grieco@unina.it.

Author Contributions

A.C. and A. L. are responsible for design and NMR analysis. L.A., F.M., A.M.Y., and P.G. are responsible for the synthesis. P.C. and I.GM. are responsible for the chemical characterization of the compounds. D.M. is responsible for stability assays. P.S., S. M., and C.A.M. are responsible for biological assays. A.C., E.N., and P.G. wrote the manuscript.

Notes

The authors declare no competing financial interest.

■ ACKNOWLEDGMENTS

The LC−MS and NMR spectral data were provided by Centro di Servizio Interdipartimentale di Analisi Strumentale (CSIAS), Università degli Studi di Napoli "Federico II". The assistance of the staff is gratefully appreciated. Part of this work was supported by Italian Ministry of Education, University and Research (PRIN-2008TSWB8K_002, PRIN2009EL5WBP_004, PRIN-2010MCLBCZ_002) and a grant from "Regione Campania"-Laboratori Pubblici progetto "Hauteville".

■ ABBREVIATIONS USED

Abbreviations used for amino acids and designation of peptides follow the rules of the IUPAC-IUB Commission of Biochemical Nomenclature in *J. Biol. Chem.* **1972**, *247*, 977−983 (amino acid symbols denote the L-configuration unless indicated otherwise); 1D, 2D, and 3D, one-, two-, and three-dimensional; Btz, benzothiazolyl-alanine; DCM, dichloromethane; DIEA, *N,N*-diisopropylethylamine; DMSO, dimethyl sulfoxide; DQF-COSY, double quantum filtered correlated spectroscopy; DPC, dodecylphosphocholine; EM, energy minimization; FCS, fetal calf serum; FLIPR^{TETRA}, a high-throughput cellular screening system; HBTU, *N,N,N′,N′*-tetramethyl-*O*-(1*H*-benzotriazol-1-yl)uronium hexafluorophosphate; HOBt, 1-hydroxybenzotriazole; MD, molecular dynamic; Nal, naphthylalanine; NOESY, nuclear Overhauser enhancement spectroscopy; NOE, nuclear Overhauser effect; NMR, nuclear magnetic resonance; Orn, ornithine; Pen, penicillamine; SDS, sodium dodecylsulfate; SAR, structure−activity relationship; TFA, trifluoroacetic acid; TOCSY, total correlated spectroscopy; Trt, triphenylmethyl; TSP, 3-(trimethylsilanyl)propionic acid; UT, urotensin II receptor; *h*-UT, human urotensin II receptor; U-II, urotensin-II peptide; *h*U-II, human urotensin-II peptide.

■ REFERENCES

(1) (a) Bern, H. A.; Lederis, K. A Reference Preparation for the Study of Active Substances in the Caudal Neurosecretory System of Teleosts. *J. Endrocninol.* **1969**, *45* (Suppl.), xi−xii. (b) Pearson, D.; Shively, J. E.; Clark, B. R.; Geschwind, I. I.; Barkley, M.; Nishioka, R. S.; Bern, H. A. Urotensin II: A Somatostain-like Peptide in the Caudal Neurosecretory System of Fishes. *Proc. Natl. Acad. Sci. U.S.A.* **1980**, *77*, 5021−5024.

(2) Conlon, J. M.; O'Harte, F.; Smith, D. D.; Tonon, M. C.; Vaudry, H. Isolation and Primary Structure of Urotensin II From the Brain of a Tetrapod, the Frog *Rana ridibunda*. *Biochem. Biophys. Res. Commun.* **1992**, *188*, 578−583.

(3) Mori, M.; Sugo, T.; Abe, M.; Shimomura, Y.; Kurihara, M.; Kitada, C.; Kikuchi, K.; Shintani, Y.; Kurokawa, T.; Onda, H.; Nishimura, O.; Fujino, M. Urotensin II is the Endogenous Ligand of a G-protein Coupled Orphan Receptor, SENR (GPR14). *Biochem. Biophys. Res. Commun.* **1999**, *265*, 123−129.

(4) Nothacker, H. P.; Wang, Z.; McNeill, A. M.; Saito, Y.; Merten, S.; O'Dowd, B.; Duckles, S. P.; Civelli, O. Identification of the Natural Ligand of an Orphan G-Protein-Coupled Receptor Involved in the Regulation of Vasoconstriction. *Nat. Cell Biol.* **1999**, *1*, 383−385.

(5) Ames, R. S.; Sarau, H. M.; Chambers, J. K.; Willette, R. N.; Aiyar, R. V.; Romanic, A. M.; Louden, C. S.; Foley, J. J.; Sauermelch, C. F.; Coatney, R. W.; Ao, Z.; Disa, J.; Holmes, S. D.; Stadel, J. M.; Martin, J. D.; Liu, W.-S.; Glover, G. I.; Wilson, S.; McNutty, D. E.; Ellis, C. E.; Eishourbagy, N. A.; Shabon, U.; Trill, J. J.; Hay, D. V. P.; Ohlstein, E. H.; Bergsma, D. J.; Douglas, S. A. Human Urotensin-II Is a Potent Vasoconstrictor and Agonist for the Orphan Receptor GPR14. *Nature* **1999**, *401*, 282−286.

(6) Vaudry, H.; Do Rego, J. C.; Le Mevel, J. C.; Chatenet, D.; Tostivint, H.; Fournier, A.; Tonon, M. C.; Pelletier, G.; Conlon, J. M.; Leprince, J. Urotensin II, from Fish to Human. *Ann. N.Y. Acad. Sci.* **2010**, *200*, 53−66.

(7) Sugo, T.; Murakami, Y.; Shimomura, Y.; Harada, M.; Abe, M.; Ishibashi, Y.; Kitada, C.; Miyajima, N.; Suzuki, N.; Mori, M.; Fujino, M. Identification of Urotensin II-Related Peptide as the Urotensin II Immunoreactive Molecule in the Rat Brain. *Biochem. Biophys. Res. Commun.* **2003**, *310*, 860−868.

(8) (a) Maguire, J. J.; Kuc, R. E.; Davenport, A. P. Orphan-Receptor Ligand Human Urotensin II: Receptor Localization Human Tissues and Comparison of Vasoconstrictor Responses with Endothelin-1. *Br. J. Pharmacol.* **2000**, *131*, 441−446. (b) Maguire, J. J.; Davenport, A. P. Is Urotensin-II the New Endothelin? *Br. J. Pharmacol.* **2002**, *137*, 579−588.

(9) Matsushita, M.; Shichiri, M.; Imai, T.; Iwashina, M.; Tanaka, H.; Takasu, N.; Hirata, Y. Co-Expression of Urotensin II and Its Receptor (GPR14) in Human Cardiovascular and Renal Tissues. *J. Hypertens.* **2001**, *19*, 2185−2190.

(10) Zhu, Y. C.; Zhu, Y. Z.; Moore, P. K. The Role of Urotensin II in Cardiovascular and Renal Physiology and Diseases. *Br. J. Pharmacol.* **2006**, *148*, 884−901.

(11) (a) Suzuki, S.; Wenyi, Z.; Hirai, M.; Hinokio, Y.; Suzuki, C.; Yamada, T.; Yoshizumi, S.; Suzuki, M.; Tanizawa, Y.; Matsutani, A.; Oka, Y. Genetic Variations at Urotensin II and Urotensin II Receptor Genes and Risk of Type 2 Diabetes Mellitus in Japanese. *Peptides* **2004**, *25*, 1803−1808. (b) Douglas, S. A.; Ohlstein, E. H. Human Urotensin-II, the Most Potent Mammalian Vasoconstrictor Identified to Date, as a Therapeutic Target for the Management of Cardivascular Diseases. *Trends Cardiovasc. Med.* **2000**, *10*, 229−237. (c) Douglas, S. A. Human Urotensin-II as a Novel Cardiovascular Target: "Heart" of the Matter or Simply a Fish "Tail"? *Curr. Opin. Pharmacol.* **2003**, *3*, 159−167. (d) Papadopoulos, P.; Bousette, N.; Giaid, A. Urotensin-II and Cardiovascular Remodeling. *Peptides* **2008**, *29*, 764−769.

(12) Djordjevic, T.; Belaiba, R. S.; Bonello, S.; Pfeilschifter, J.; Hess, J.; Gorlach, A. Human Urotensin II Is a Novel Activator of NADPH Oxidase in Human Pulmonary Artery Smooth Muscle Cells. *Arterioscler. Thromb. Vasc. Biol.* **2005**, *25*, 519−25.
(13) (a) d'Emmanuele di Villa Bianca, R.; Mitidieri, E.; Coletta, C.; Grassia, G.; Roviezzo, F.; Grieco, P.; Novellino, E.; Imbimbo, C.; Mirone, V.; Cirino, P.; Sorrentino, R. Urotensin II: A Novel Target in Human Penile Erection. *J. Sex. Med.* **2010**, *7*, 1178−1186. (b) d'Emmanuele di Villa Bianca, R.; Mitidieri, E.; Fusco, F.; D'Aiuto, E.; Grieco, P.; Novellino, E.; Imbimbo, C.; Mirone, V.; Cirino, G.; Sorrentino, R. Endogenous Urotensin II Selectively Modulates Erectile Function through eNOS. *PLoS One* **2012**, *7*, e31019.
(14) Grieco, P.; Franco, R.; Bozzuto, G.; Toccacieli, L.; Sgambato, A.; Marra, M.; Zappavigna, S.; Migaldi, M.; Rossi, G.; Striano, S.; Marra, L.; Gallo, L.; Cittadini, A.; Botti, G.; Novellino, E.; Molinari, A.; Budillon, A.; Caraglia, M. Urotensin II Receptor Predicts the Clinical Outcome of Prostate Cancer Patients and Is Involved in the Regulation of Motility of Prostate Adenocarcinoma Cells. *J. Cell Biochem.* **2011**, *112*, 341−353.
(15) Liang, D. Y.; Liu, L. M.; Ye, C. G.; Zhao, L.; Yu, F. P.; Gao, D. Y.; Wang, Y. Y.; Yang, Z. W.; Wang, Y. Y. Inhibition of UII/UTR System Relieves Acute Inflammation of Liver through Preventing Activation of NF-κB Pathway in ALF Mice. *PLoS One* **2013**, *8*, e64895.
(16) Matsumoto, Y.; Abe, M.; Watanabe, T.; Adachi, Y.; Yano, T.; Takahashi, H.; Sugo, T.; Mori, M.; Kitada, C.; Kurokawa, T.; Fujino, M. Intracerebroventricular Administration of Urotensin II Promotes Anxiogenic-like Behaviors in Rodents. *Neurosci. Lett.* **2004**, *358*, 99−102.
(17) (a) Chatenet, D.; Nguyen, T. T.; Létourneau, M.; Fournier, A. Update on the Urotensinergic System: New Trends in Receptor Localization, Activation, and Drug Design. *Front Endocrinol.* **2013**, *3*, 1−13. (b) Maryanoff, B. E.; Kinney, W. A. Urotensin-II Receptor Modulators as Potential Drugs. *J. Med. Chem.* **2010**, *53*, 2695−2708.
(18) Conlon, J. M.; Yano, K.; Waugh, D.; Hazon, N. Distribution and Molecular Forms of Urotensin II and Its Role in Cardiovascular Regulation in Vertebrates. *J. Exp. Zool.* **1996**, *275*, 226−238.
(19) Chatenet, D.; Dubessy, C.; Leprince, J.; Boularan, C.; Carlier, L.; Segalas-Milazzo, I.; Guilhaudis, L.; Oulyadi, H.; Davoust, D.; Scalbert, E.; Pfeiffer, B.; Renard, P.; Tonon, M. C.; Lihrmann, I.; Pacaud, P.; Vaudry, H. Structure−Activity Relationships and Structural Conformation of a Novel Urotensin II-Related Peptide. *Peptides* **2004**, *25*, 1819−1830.
(20) Flohr, S.; Kurz, M.; Kostenis, E.; Brkovich, A.; Fournier, A.; Klabunde, T. Identification of Nonpeptidic Urotensin II Receptor Antagonists by Virtual Screening Based on a Pharmacophore Model Derived from Structure−Activity Relationships and Nuclear Magnetic Resonance Studies on Urotensin II. *J. Med. Chem.* **2002**, *45*, 1799−1805.
(21) Kinney, W. A.; Almond, H. R.; Qi, J.; Smith, C. E.; Santulli, R. J.; de Garavilla, L.; Andrade-Gordon, P.; Cho, D. S.; Everson, A. M.; Feinstein, M. A.; Leung, P. A.; Maryanoff, B. E. Structure−Function Analysis of Urotensin II and Its Use in the Construction of a Ligand−Receptor Working Model. *Angew. Chem., Int. Ed.* **2002**, *41*, 2940−2944.
(22) Brkovic, A.; Hattenberger, A.; Kostenis, E.; Klabunde, T.; Flohr, S.; Kurz, M.; Bourgault, S.; Fournier, A. Functional and Binding Characterizations of Urotensin II-Related Peptides in Human and Rat Urotensin II-Receptor Assay. *J. Pharmacol. Exp. Ther.* **2003**, *306*, 1200−1209.
(23) Labarrere, P.; Chatenet, D.; Leprince, J.; Marionneau, C.; Loirand, G.; Tonon, M. C.; Dubessy, C.; Scalbert, E.; Pfeiffer, B.; Renard, P.; Calas, B.; Pacaud, P.; Vaudry, H. Structure−Activity Relationships of Human Urotensin II and Related Analogues on Rat Aortic Ring Contraction. *J. Enz. Inhib. Med. Chem.* **2003**, *18*, 77−88.
(24) Coy, D. H.; Rossowski, W. J.; Cheng, B. L.; Taylor, J. E. Structural Requirements at the N-Terminus of Urotensin II Octapeptides. *Peptides* **2002**, *23*, 2259−2264.
(25) Grieco, P.; Carotenuto, A.; Campiglia, P.; Zampelli, E.; Patacchini, R.; Maggi, C. A.; Novellino, E.; Rovero, P. A New Potent Urotensin-II Receptor Peptide Agonist Containing a Pen Residue at Disulfide Bridge. *J. Med. Chem.* **2002**, *45*, 4391−4394.
(26) Patacchini, R.; Santicioli, P.; Giuliani, S.; Grieco, P.; Novellino, E.; Rovero, P.; Maggi, C. A. Urantide: An Ultrapotent Urotensin II Antagonist Peptide in the Rat Aorta. *Br. J. Pharmacol.* **2003**, *140*, 1155−1158.
(27) Zhao, J.; Yu, Q. X.; Kong, W.; Gao, H. C.; Sun, B.; Xie, Y. Q.; Ren, L. Q. The Urotensin II Receptor Antagonist, Urantide, Protects against Atherosclerosis in Rats. *Exp. Ther. Med.* **2013**, *5*, 1765−1769.
(28) Grieco, P.; Carotenuto, A.; Campiglia, P.; Gomez-Monterrey, I.; Auriemma, L.; Sala, M.; Marcozzi, C.; d'Emmanuele di Villa Bianca, R.; Brancaccio, D.; Rovero, P.; Santicioli, P.; Meini, S.; Maggi, C. A.; Novellino, E. New Insight into the Binding Mode of Peptide Ligands at Urotensin-II Receptor: Structure−Activity Relationships Study on P5U and Urantide. *J. Med. Chem.* **2009**, *52*, 3927−3940.
(29) Grieco, P.; Carotenuto, A.; Patacchini, R.; Maggi, C. A.; Novellino, E.; Rovero, P. Design, Synthesis, Conformational Analysis, and Biological Studies of Urotensin II Lactam Analogues. *Bioorg. Med. Chem.* **2002**, *10*, 3731−3739.
(30) (a) Novellino, E.; Grieco, P.; Rovero, P. Cyclic Peptides Acting as Urotensin II Antagonists, and Use in the Treatment of Hypertension and Other Cardiovascular Conditions and in Urotensin II Receptor Characterization. PCT Int. Appl. WO 2005023845 A2 20050317, 2005. (b) Pitaro, M.; Chiarella, A. Peptidi Ciclici Sintetici Agonisti ed Antagonisti dell'Urotensina II e Relative Procedimento di Produzione. Italian Patent RM2013A000470.
(31) Carotenuto, A.; Auriemma, L.; Merlino, F.; Limatola, A.; Campiglia, P.; Gomez-Monterrey, I.; d'Emmanuele di Villa Bianca, R.; Brancaccio, D.; Santicioli, P.; Meini, S.; Maggi, C. A.; Novellino, E.; Grieco, P. New Insight into the Binding Mode of Peptides at Urotensin-II Receptor by Trp-Constrained Analogues of P5U and Urantide. *J. Pept. Sci.* **2013**, *5*, 293−300.
(32) (a) Fernandez-Lopez, S.; Kim, H. S.; Choi, E. C.; Delgado, M.; Granja, J. R.; Khasanov, A.; Kraehenbuehl, K.; Long, G.; Weinberger, D. A.; Wilcoxen, K. M.; Ghadiri, M. R. Antibacterial Agents Based on the Cyclic D,L-Alpha-Peptide Architecture. *Nature* **2001**, *412*, 452−455; Erratum. *Nature* **2001**, *414*, 329. (b) Chan, L. Y.; Gunasekera, S.; Henriques, S. T.; Worth, N. F.; Le, S. J.; Clark, R. J.; Campbell, J. H.; Craik, D. J.; Daly, N. L. Engineering Pro-Angiogenic Peptides Using Stable, Disulfide-Rich Cyclic Scaffolds. *Blood* **2011**, *118*, 6709−6717.
(33) Carotenuto, A.; Grieco, P.; Campiglia, P.; Novellino, E.; Rovero, P. Unraveling the Active Conformation of Urotensin II. *J. Med. Chem.* **2004**, *47*, 1652−1661.
(34) Grieco, P.; Carotenuto, A.; Campiglia, P.; Marinelli, L.; Lama, T.; Patacchini, R.; Santicioli, P.; Maggi, C. A.; Rovero, P.; Novellino, E. Urotensin-II Receptor Ligands. From Agonist to Antagonist Activity. *J. Med. Chem.* **2005**, *48*, 7290−7297.
(35) Di Cianni, A.; Carotenuto, A.; Brancaccio, D.; Novellino, E.; Reubi, J. C.; Beetschen, K.; Papini, A. M.; Ginanneschi, M. Novel Octreotide Dicarba-Analogues with High Affinity and Different Selectivity for Somatostatin Receptors. *J. Med. Chem.* **2010**, *53*, 6188−6197.
(36) Saviello, M. R.; Malfi, S.; Campiglia, P.; Cavalli, A.; Grieco, P.; Novellino, E.; Carotenuto, A. New Insight into the Mechanism of Action of the Antimicrobial Peptides Temporins. *Biochemistry* **2010**, *49*, 1477−1485.
(37) Wüthrich, K. In *NMR of Proteins and Nucleic Acids*; John Wiley & Sons: New York, 1986.
(38) (a) Carotenuto, A.; Grieco, P.; Rovero, P.; Novellino, E. Urotensin-II Receptor Antagonists. *Curr. Med. Chem.* **2006**, *13*, 267−275. (b) Guerrini, R.; Camarda, V.; Marzola, E.; Arduin, M.; Calo, G.; Spagnol, M.; Rizzi, A.; Salvadori, S.; Regoli, D. Structure−Activity Relationship Study on Human Urotensin II. *J. Pept. Sci.* **2005**, *2*, 85−90. (c) Chatenet, D.; Dubessy, C.; Boularan, C.; Scalbert, E.; Pfeiffer, B.; Renard, P.; Lihrmann, I.; Pacaud, P.; Tonon, M. C.; Vaudry, H.; Leprince, J. Structure−Activity Relationships of a Novel Series of Urotensin II Analogues: Identification of an Urotensin II Antagonist. *J. Med. Chem.* **2006**, *49*, 7234−7238. (d) Leprince, J.; Chatenet, D.; Dubessy, C.; Fournier, A.; Pfeiffer, B.; Scalbert, E.; Renard, P.; Pacaud, P.; Oulyadi, H.; Ségalas-Milazzo, I.; Guilhaudis, L.; Davoust, D.; Tonon,

M. C.; Vaudry, H. Structure−Activity Relationships of Urotensin II and URP. *Peptides* **2008**, *5*, 658−673.
(39) Batuwangala, M.; Camarda, V.; McDonald, J.; Marzola, E.; Lambert, D. G.; Ng, L. L.; Calò, G.; Regoli, D.; Trapella, C.; Guerrini, R.; Salvadori, S. *Peptides* **2009**, *30*, 1130−1136.
(40) Camarda, V.; Song, W.; Marzola, E.; Spagnol, M.; Guerrini, R.; Salvatori, S.; Regoli, D.; Thompson, J. P.; Rowbotham, D. J.; Behm, D. J.; Douglas, S. A.; Calo', G.; Lambert, D. G. Urantide Mimics Urotensin-II Induced Calcium Release in Cells Expressing Recombinant UT Receptors. *Eur. J. Pharmacol.* **2004**, *498*, 83−86.
(41) (a) Chen, Z.; Xu, J.; Ye, Y.; Li, Y.; Gong, H.; Zhang, G.; Wu, J.; jia, J.; Liu, M.; Chen, Y.; Yang, C.; Tang, Y.; Zhu, Z.; Ge, J.; Zou, Y. Urotensin II Inhibited the Proliferation of Cardiac Side Population Cells in Mice during Pressure Overload by JNK-LRP6 Signalling. *J. Cell. Mol. Med.* **2014**, DOI: 10.1111/jcmm.12230. (b) Gao, S.; Oh, Y. B.; Shah, A.; Park, W. H.; Chung, M. J.; Lee, Y. H.; Kim, S. H. Urotensin II Receptor Antagonist Attenuates Monocrotaline-Induced Cardiac Hypertrophy in Rats. *Am. J. Physiol. Heart Circ. Physiol.* **2010**, *299*, H1782−1789. (c) Zhang, J. Y.; Chen, Z. W.; Yao, H. Protective Effect of Urantide Against Ischemia-Reperfusion Injury via Protein Kinase C and Phosphtidylinositol 3′-Kinase-Akt Pathway. *Can. J. Physiol. Pharmacol.* **2012**, *90*, 637−645.
(42) Brancaccio, D.; Limatola, A.; Campiglia, P.; Gomez-Monterrey, I.; Novellino, E.; Grieco, P.; Carotenuto, A. Urantide Conformation and Interaction with Urotensin-II Receptor. *Arch. Pharm.* **2013**, *246*, 1−8.
(43) Stewart, J. M.; Young, J. D. In *Solid Phase Peptide Synthesis*; Pierce Chemical: Rockford, IL, 1984.
(44) (a) Wang, S. S.; Tam, J. P.; Wang, B. S.; Merrifield, R. B. Enhancement of Peptide Coupling Reactions by 4-Dimethylaminopyridine. *Int. J. Pept. Protein Res.* **1981**, *18*, 459−467. (b) Atherton, E.; Sheppard, R. C. *Solid-Phase Peptide Synthesis: A Practical Approach*; IRL Press: Oxford, U.K., 1989.
(45) Misika, A.; Hruby, V. J. Optimization of Disulfide Bond Formation. *Polym. J. Chem.* **1994**, *68*, 893−899.
(46) (a) Kenakin, T. Orthosteric Drug Antagonism. In *A Pharmacology Primer: Theory, Application, and Methods*, 2nd ed.; Elsevier, Academic Press: London, UK, 2006; pp 99−126. (b) Arunlakshana, O.; Schild, H. O. Some Quantitative Uses of Drug Antagonists. *Br. J. Pharmacol. Chemother.* **1959**, *14*, 48−58. (c) Cheng, Y.; Prusoff, W. H. Relationship Between the Inhibition Constant (Ki) and the Concentration of Inhibitor which Causes 50 per Cent Inhibition (I_{50}) of an Enzymatic Reaction. *Biochem. Pharmacol.* **1973**, *22*, 3099−3108.
(47) Riddy, D. M.; Stamp, C.; Sykes, D. A.; Charlton, S. J.; Dowling, M. R. Reassessment of the Pharmacology of Sphingosine-1-phosphate S1P3 Receptor Ligands Using the DiscoveRx PathHunter and Ca^{2+} Release Functional Assays. *Br. J. Pharmacol.* **2012**, *167*, 868−880.
(48) (a) Nguyen, L. T.; Chau, J. K.; Perry, N. A.; de Boer, L.; Zaat, S. A.; Vogel, H. J. Serum Stabilities of Short Tryptophan- and Arginine-Rich Antimicrobial Peptide Analogs. *PLoS One* **2010**, *5*, e12684. (b) Doti, N.; Scognamiglio, P. L.; Madonna, S.; Scarponi, C.; Ruvo, M.; Perretta, G.; Albanesi, C.; Marasco, D. New Mimetic Peptides of the Kinase-Inhibitory Region (KIR) of SOCS1 through Focused Peptide Libraries. *Biochem. J.* **2012**, *443*, 231−240.
(49) Hwang, T. L.; Shaka, A. J. Water Suppression That Works. Excitation Sculpting Using Arbitrary Wave-Forms and Pulsed-Field Gradients. *J. Magn. Reson.* **1995**, *112*, 275−279.
(50) (a) Piantini, U.; Sorensen, O. W.; Ernst, R. R. Multiple Quantum Filters for Elucidating NMR Coupling Network. *J. Am. Chem. Soc.* **1982**, *104*, 6800−6801. (b) Marion, D.; Wüthrich, K. Application of Phase Sensitive Two-Dimensional Correlated Spectroscopy (COSY) for Measurements of $^1H-^1H$ Spin−Spin Coupling Constants in Proteins. *Biochem. Biophys. Res. Commun.* **1983**, *113*, 967−974.
(51) Braunschweiler, L.; Ernst, R. R. Coherence Transfer by Isotropic Mixing: Application to Proton Correlation Spectroscopy. *J. Magn. Reson.* **1983**, *53*, 521−528.
(52) Jenner, J.; Meyer, B. H.; Bachman, P.; Ernst, R. R. Investigation of Exchange Processes by Two-Dimensional NMR Spectroscopy. *J. Chem. Phys.* **1979**, *71*, 4546−4553.
(53) States, D. J.; Haberkorn, R. A.; Ruben, D. J. A Two-Dimensional Nuclear Overhauser Experiment with Pure Absorption Phase in Four Quadrants. *J. Magn. Reson.* **1982**, *48*, 286−292.
(54) Bartels, C.; Xia, T.; Billeter, M.; Guentert, P.; Wüthrich, K. The Program XEASY for Computer-Supported NMR Spectral Analysis of Biological Macromolecules. *J. Biomol. NMR* **1995**, *6*, 1−10.
(55) Güntert, P.; Mumenthaler, C.; Wüthrich, K. Torsion Angle Dynamics for NMR Structure Calculation with the New Program DYANA. *J. Mol. Biol.* **1997**, *273*, 283−298.
(56) Koradi, R.; Billeter, M.; Wüthrich, K. MOLMOL: A Program for Display and Analysis of Macromolecular Structures. *J. Mol. Graphics* **1996**, *14*, 51−55.
(57) Maple, J.; Dinur, U.; Hagler, A. T. Derivation of Force Fields for Molecular Mechanics and Dynamics from Ab Initio Energy Surface. *Proc. Natl. Acad. Sci. U. S. A.* **1988**, *85*, 5350−5354.